ISSN 1061-8309, Russian Journal of Nondestructive Testing, 2014, Vol. 50, No. 2, pp. 120–126. © Pleiades Publishing, Ltd., 2014.
Original Russian Text © V.R. Skal'skii, I.M. Lyasota, 2014, published in Defektoskopiya, 2014, Vol. 50, No. 2, pp. 79–86.

ACOUSTIC METHODS

Features of Acoustic-Emission Signals during the Initiation of a Fatigue Failure in a Welded Joint of an Aluminum Alloy of the Al–Cu–Mn System

V. R. Skal'skii and I. M. Lyasota

Karpenko Physical–Mechanical Institute, National Academy of Sciences of Ukraine, 5, Naukova str. Lviv, 79601, Ukraine

e-mail: skal@imp.lviv.ua; lyasota_igor@yahoo.com

Received March 21, 2013

Abstract—The features of the generation of acoustic emissions (AEs) during the initiation of a fatigue failure in various zones of a welded joint of thermally hardened 2219-T6-grade aluminum alloy, which is produced using electron-beam welding, are considered. Metallographic studies showed that a welded joint of the alloy is structurally and mechanically inhomogeneous. This predominantly influences the initiation and development kinetics of fatigue cracks in the joint and the AE kinetics. It is shown that the area of a formed flaw is proportional to the sum of the amplitude of detected signals, and the transition from the initiation to the stable propagation of a failure is accompanied by an abrupt increase in AE activity.

Keywords: aluminum alloy, welded joints, acoustic emission, microstructure, fatigue crack

DOI: 10.1134/S1061830914020077

High-strength aluminum alloys (AAs) are successfully used virtually in all fields of science and technology, including aerospace engineering, owing to their set of physicomechanical, corrosion, and technological properties. Critical aluminum elements of aircraft (fuel tanks of rockets, the elements of a spaceship cabin module, etc.) are connected using electron-beam welding, because this technology provides high-quality thick-wall welded joints (WJs). During long operation under the actions of different factors, including alternating loading, micro- and macrofractures often originate in the elements of constructions containing AAs and their WJs. As has been established from statistical studies, the development of fatigue cracks is the most widespread factor that causes failures in spacecraft [1], thus stimulating improvements in their diagnostic techniques. Owing to the high accuracy and the possibility of monitoring the development of a flaw in real time, the acoustic-emission (AE) method efficiently detects propagation of damage [1–14, 20]. However, it has seldom been used to determine the fatigue strength of welded AA joints. Therefore, in order to perform the high-quality AE diagnostics of the state of aluminum elements of structures, it is important to know the activity and specific features of AE signals during the initiation and development of fatigue-failure processes.

The objective of this study was to investigate the features of AE generation during the propagation of fatigue cracks in different zones of WJs in an alloy of the Al–Cu–Mn system, which are produced using electron-beam welding.

Reviews of the literature sources that are devoted to the AE diagnostics of fatigue failures of metallic alloys were published in [2, 3].

One of the first studies in this field was performed by Harris et al. in 1974 [4]. The essence of these experiments involved observations of the generated AE during the propagation of fatigue cracks in the 7075-76 Al alloy (the Al–Cu–Mn alloy system). The relationships between the crack growth, the stress intensity factor, and the parameters of AE signals were established in experiments. It was shown that this method allows the detection of crack initiation, even when its propagation rate is lower than 10^{-6} m/cycle, and the total AE count is closely related to the energy that is released during the crack propagation within a single loading cycle. Analogous results were also obtained in [5], where AE was studied during the fatigue-induced failure of compact steel specimens. Here, the AEs were registered when the maximum load in a cycle was attained, and only such signals were perceived that were generated by a crack growth but not by the friction of its edges.

Table 1. The chemical composition of the 2219-T alloy (wt %) [15]

Al	Cu	Mn	Zr	Ti	V	Si	Fe	Mg	Zn	Other impurities
						at most				
Base	5.8–6.8	0.2–0.4	0.1–0.25	0.02–0.1	0.05–0.15	0.2	0.3	0.02	0.1	0.15

The kinetics of the propagation of short and long fatigue cracks in welded steel seams [6] and in the LY12CZ aluminum alloy of the Al–Cu–Mg–Mn system [7] have been investigated using the AE-source location technique [6, 7]. The obtained data were used to construct kinetic fatigue-failure diagrams for different values of the cycle asymmetry in the range $R = 0.1–0.7$. It was established that for identical load values, the growth rate of a short crack is much higher than the growth rate of a long crack. Typical wave representations of AE signals and their spectral distributions, which were obtained during propagation of cracks of both types, are also shown. The signals from both cracks were similar, but the amplitudes of the signals that were generated by the propagation of long cracks were larger by a factor of >2.

The authors of [1] studied the features of the AEs that were radiated during the fatigue failure of plates with dimensions of 750 × 300 × 2 mm manufactured of an aircraft-grade aluminum alloy. AEs were detected with four resonance transducers with an operating frequency of 150 kHz. The dependences of the change in the total AE count on the number of loading cycles showed that the transition from the fatigue-crack initiation to its stable propagation is accompanied by an abrupt increase in the AE activity.

Similar studies were performed in [8], where the AE features were monitored during the fatigue failure of compact specimens of the 7075 aluminum alloy. The *RA* criterion, which is equal to the ratio of the rise time of the leading edge of the AE signal to its amplitude, was used to evaluate the damage propagation. It was established that the parameter *RA* sharply increases upon a change to the supercritical crack-development stage; this is about 1000 cycles to the complete specimen destruction. The time-dependent change in the coefficient *RA* properly correlates with the crack-growth curve.

The AE features during the fatigue failure of the 6082-T6 aluminum alloy (the Al–Mg–Si alloy system) were described in [9]. As in previous investigations, in order to avoid the reflection of elastic AE waves from the surfaces of a body, large specimens with dimensions of 1200 × 1000 × 3 mm were used. The loading frequency was only 1 Hz, thus allowing efficient detection of AE signals from each jumpwise crack increase. The experimental data were used to construct a finite-element 3D model of generation of elastic AE waves during propagation of a fatigue crack.

When studying the AE behavior kinetics during propagation of a fatigue crack in the incoloy 901 alloy, it was found [10] that the dependence of the change in the total AE count on the number of loading cycles contains three damage-development stages: initiation, stable propagation, and the supercritical stage (specimen rupture). An abrupt AE-activity jump is observed during the transition to each subsequent stage. A pattern similar to that in previous studies was observed in [11] during cyclic tensile loading of cylindrical specimens of the ultimet alloy. The dependence of the change in the total AE count on the number of loading cycles has a stepwise character [11]. The authors assert that an abrupt periodic increase in the AE activity indicates a stepwise growth of a macrocrack, and during the so-called "incubation" period (formation of a plastic zone near the crack tip) between AE pulses, small-amplitude AE pulses are generated.

Investigations devoted to the identification of AE sources for an aluminum alloy in a fatigue state have been performed [12–14]. Using the spectral characteristics of AE signals and fractographic studies, it was established that the main AE generation source is the fracture of brittle intermetallic inclusions located near the crack tip [12]. The fraction of these AE signals is 80% of all detected signals and their amplitude and intensity depend on the shape, size, and spatial localizations of inclusions [13].

Thus, analysis of the literature shows that the problem of studying the influence of the structural and mechanical inhomogeneities of thick-wall aluminum-alloy WJs on the generation of AE signals during propagation of fatigue cracks in them has not been comprehensively studied.

Features of the microstructure of a WJ in the 2219-T6 alloy. The effective AE diagnostics of a fatigue failure requires knowledge of the specific features of the base-metal microstructure and characteristic areas of a WJ. For this purpose, an EVO-40XVP scanning electron microscope was used. When the chemical element-by-element analysis was performed, the voltage that accelerated the electron beam was 20 keV.

The thermally hardened 2219-T6 aluminum alloy (which is known as the 1201-T6 grade alloy) refers to the Al–Cu–Mn alloy system. The chemical composition of the alloy is presented in Table 1. At room

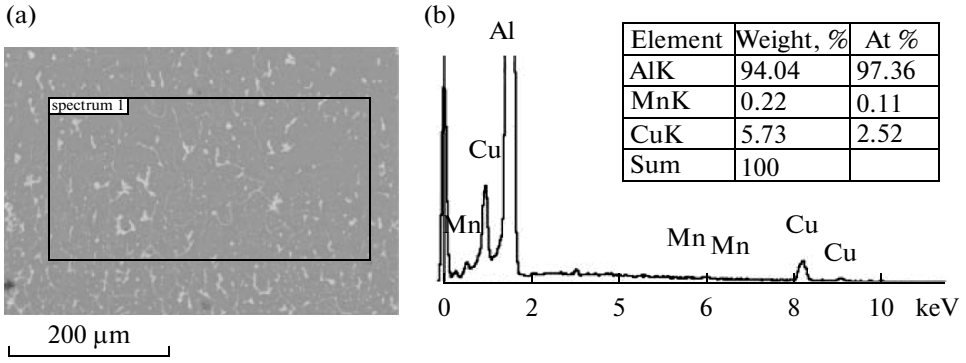

Element	Weight, %	At %
AlK	94.04	97.36
MnK	0.22	0.11
CuK	5.73	2.52
Sum	100	

Fig. 1. (a) The microstructure and (b) EDS spectrum of the element distribution in the base metal of the 2219-T6 alloy.

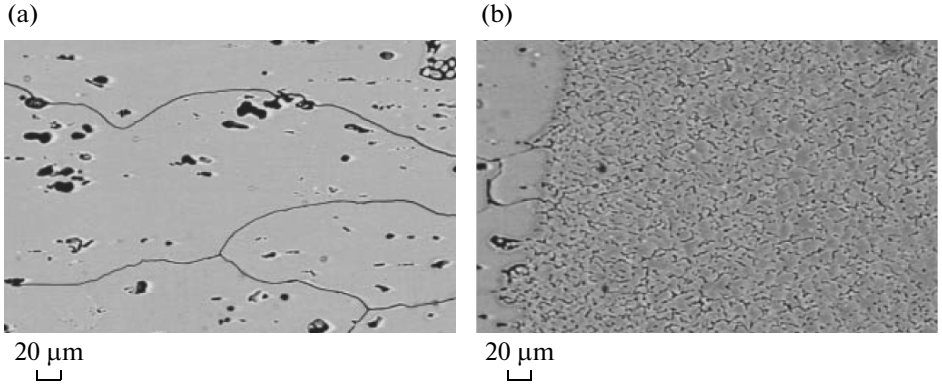

Fig. 2. (a) The microstructures of the TEZ and (b) the seam metal of a WJ of the 2219-T6 alloy produced using electron-beam welding.

temperature, its microstructure consists of grains whose body is composed of an α solid solution of copper and manganese in aluminum and secondary θ (Al_2Cu) and T ($Al_{12}Mn_2Cu$) phases, which are uniformly distributed over a grain in the form of fine needle-shaped inclusions and also along the grain boundaries in the form of large flakes (Fig. 1).

AAs of this grade are characterized by a significant disintegration of the α solid solution during welding; therefore, in the heat-affected zone (HAZ), structural transformations occur already at $T = 673$ K and higher, which lead to an intense recrystallization growth of grains and coagulation of hardening phases at their boundaries (Fig. 2a), thus resulting in a decrease in the metal hardness [16]. Owing to the high metal-cooling rate during electron-beam welding, a seam has a finely dispersed structure (Fig. 2b), whose microhardness is almost half as high as the base-metal hardness and has a value of only 70 *HV*, and the subsequent thermal treatment of the WJ can increase this value only by 10–15% [16]. Metallographic studies showed that the WJ of the 2219-T6 alloy that was produced by the electron-beam welding technique is structurally and mechanically inhomogeneous over the entire cross section; therefore, each of its zones will have individual fracture features under cyclic loading.

The materials and technique of the AE testing. The cyclic crack resistance was studied using the scheme of cantilevered bending of prismatic beam specimens manufactured from the WJs of plates with the thickness $\delta = 20$ mm, which were produced via through electron-beam welding without an added metal. The welding heat energy was 337.3 kJ. Prismatic specimens with dimensions of $10 \times 20 \times 160$ mm of two types were studied: (I) with a cut V-type sharp notch in the thermal-effect zone and (II) in the seam metal. The structural scheme of tests is shown in Fig. 3.

The specimens were manufactured according to the requirements of [17]. The depth of the stress concentrator was $h = 4$ mm and the radius of its top curvature was $\rho = 0.2$–0.3 mm. The load changed according to a sine law at a frequency $f = 16$ Hz. The cycle asymmetry factor was $R = 0.26$. The specimens were loaded with the moment $M = 8$–24 N m. AE signals that were generated as a result of a fatigue failure were received with an AE transducer that was installed on the side surface of a specimen. To select useful signals against noise, a parallel AE channel was used [20]. Electric AE signals were amplified with preamplifiers

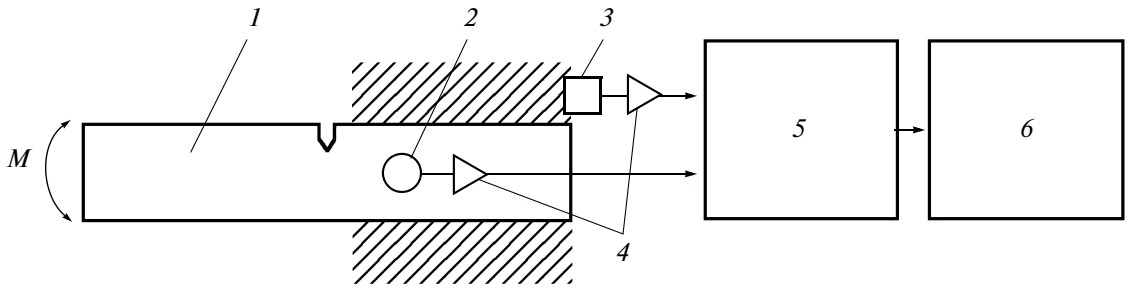

Fig. 3. A structural diagram of these experimental investigations: (*1*) specimen, (*2*) AE-sensor, (*3*) parallel AE channel of noise [18], (*4*) preamplifiers, (*5*) SKOP-8M measuring AE system, and (*6*) personal computer.

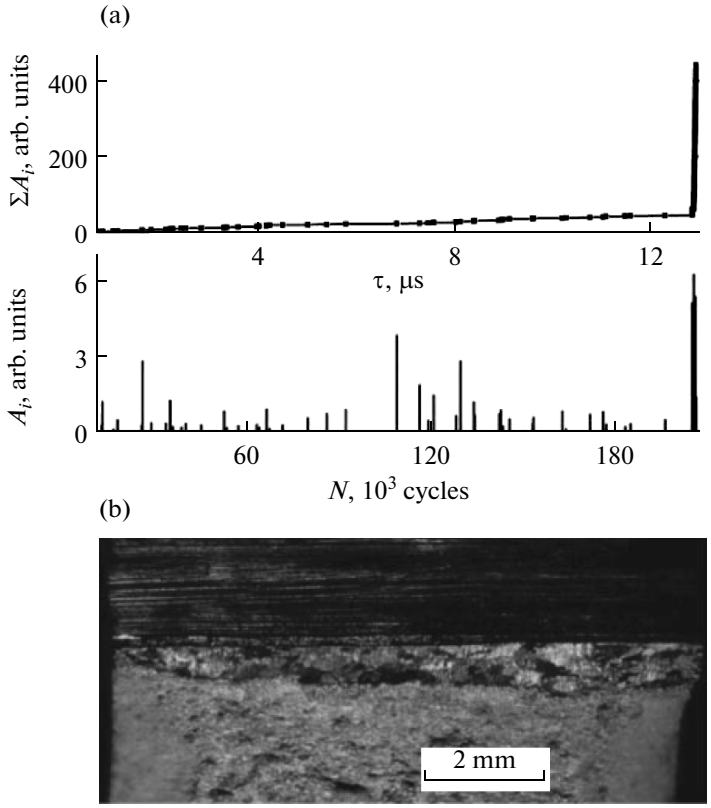

Fig. 4. (a) Changes in the amplitudes of AE signals in a sample A_i and in the sum of the amplitudes of all recorded signals within the experiment duration ΣA_i and (b) an image of a fatigue macrocrack on a metal rupture in the TEZ of welded 2219-T6 alloy joints.

4 and then recorded with a SKOP-8M multichannel measuring AE system (*5*) and processed with a personal computer (*6*). AE signals were sampled using a primary piezoelectric transducer (PET) with an operating frequency band of 0.2–0.6 MHz. Before each experiment, the sensitivity of the measuring channels was evaluated with a Gsu source [18]. The following measurement modes were set for the SKOP-8M system: the number of measuring channels for recording AE signals (the gain of each channel is 40 dB) was 2; the sampling duration was 0.25 ms; the sampling period of an analog signal was 0.25 μs; the cutoff frequencies of the low- and high-pass frequencies were 0.7 and 0.2 MHz, respectively; the discrimination threshold was 28%; and the intrinsic noise level reduced to the preamplifier input was 7 μV. The gain of the preamplifiers was 34 dB.

Test Results and Discussion

During crack initiation and propagation under the cyclic loading of specimens, the AE generation kinetics were recorded and features of the recorded signals were investigated. To measure the areas of crack

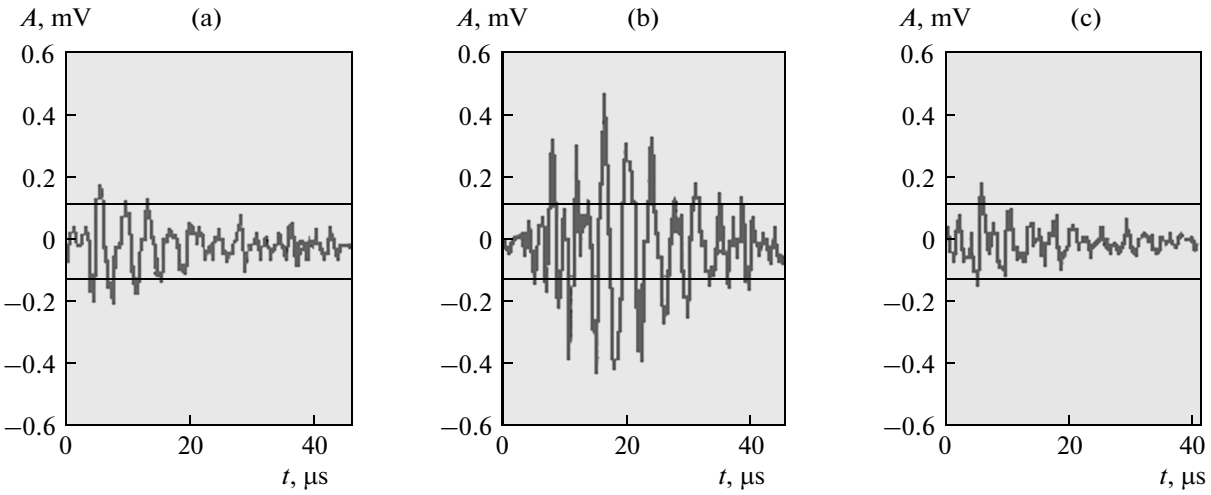

Fig. 5. Wave representations of typical AE signals during a fatigue failure: the metal in the TEZ (a) at the initiation stage and (b) during stable crack propagation, and (c) the seam metal in a WJ of the 2219-T6 alloy.

surfaces after fatigue tests, specimens were fractured at a high rate on an impact pendulum-type testing machine and the obtained ruptures were studied with an optical microscope.

It is known [19] that fatigue failures of metals and alloys occur in four stages: incubation (accumulation of the critical density of dislocations in local volumes of worked metal); accumulation of damage within separate grains; the stable growth of a crack; and an avalanche-like fracture propagation. In [20], we published the results of studies on the AE diagnostics of the fatigue failure of the base metal of the 2219-T6 alloy. It was established that earlier stages of the crack nucleation are accompanied by an insignificant number of AE signals, which are radiated in individual groups. Such an AE generation dynamics continues until the crack reaches the side surfaces of a specimen. After that, the amplitude and number of AE signals abruptly increase, thus indicating a transition to the third fracturing stage, viz., the stable propagation of the macrocrack front (the rectilinear Peris segment on the kinetic fatigue-failure diagram).

As in the base metal, the AE generation also occurs in the TEZ of welded joints. Its specific feature is that at early fatigue-failure stages, when flaws accumulate in the vicinities of local grains (the near-threshold region of the kinetic fatigue diagram), a small number of AE signals is radiated (Fig. 4b). Because the metal in the TEZ consists of large plastic recrystallized grains (Fig. 2), the AE signals that are generated upon their destruction have somewhat smaller values of the maximum amplitudes $A_i = 200–300$ μV (Fig. 5a) than those in the base metal [20]. Here, the surface of a fatigue macrocrack consists of large quasi-spalling

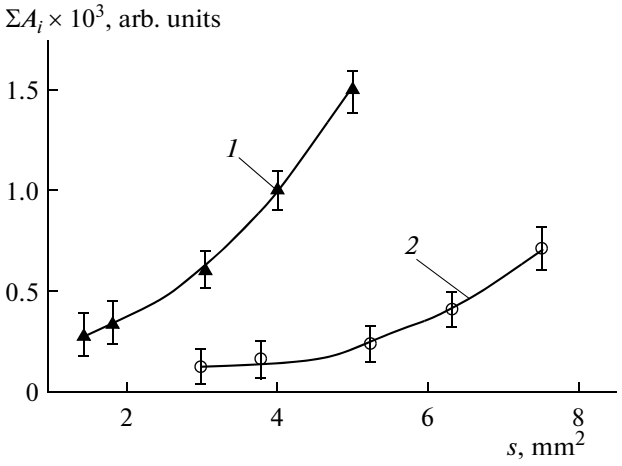

Fig. 6. The dependence of the acoustic emission signals amplitudes sum on fatigue crack area for weld metal (curve *1*) and heat-affected zone (curve *2*) 2219-T6 welding joint.

Table 2. Values of the correlation coefficients of dependence (1)

WJ zone	Numerical parameter			
	A	*B*	*C*	*r*
TEZ	551.58	−244.68	35.32	0.992
Seam metal	284.05	−165.51	69.08	0.998

planes of a transgrain fracture (Fig. 4b). The transition to the next fatigue-failure stage, viz., the stable propagation of the crack front, as in the case of the base metal [20], is accompanied by an abrupt increase in the AE activity (Fig. 4a). In this case, signals with amplitudes $A_i = 500–600$ μV are generated (Fig. 5b).

The AE radiation kinetics during fatigue fracturing of the seam metal is similar to the cases of studying the TEZ and the base metal. However, one specific feature of the seam metal is the fact that due to the high dispersity and plasticity of its structure, a large number of signals with small amplitudes $A_i = 200–250$ μV are generated in the seam. Their characteristic wave representation is shown in Fig. 5c.

The performed experiments showed that the structural and mechanical inhomogeneities of WJs of the 2219-T6 alloy, which were produced using electron-beam welding, cause different features of AE generation in each zone of a WJ. Figure 6 shows the dependences of the area of the fatigue cracks on the sum of the amplitudes of recorded AE signals, which were approximated by the power function in the form

$$\Sigma A_i(s) = A + Bs + Cs^2, \quad (1)$$

where A, B, and C are the approximation parameters, whose values for each WJ zone are presented in Table 2.

A power change in the dependences of the areas of fatigue cracks on the sum of the amplitudes of AE signals (Fig. 6), as in the case of the base metal in [20], is determined by a jumpwise increase in the AE activity upon a change of the fatigue failure from the initiation stage to its stable propagation. As is seen, the size of the structural components of different zones of the WJ substantially affects the character of AE generation. In the case of a fatigue failure of fine-grained and plastic metal in the weld seam, a large number of small-amplitude AE signals are generated; therefore, curve *1* in Fig. 6 changes more rapidly. The transcrystallite failure of coarse and partially weakened grains in the TEZ is accompanied by the emission of a small number of signals with high amplitudes. Thus, the structural factor has the strongest effect on the character of the AE during the initiation and development of the fatigue failure in different zones of a WJ in the 2219-T6 alloy.

CONCLUSIONS

The AE method allows efficient determination of the moment of fatigue-failure initiation and permits the study of its propagation dynamics in the 2216-T6 aluminum alloy and its WJs. The AE generation depends on the microstructure in each zone of a WJ.

The initiation of a fatigue crack in the TEZ metal is accompanied by a small number of AE signals with intermediate amplitudes ($A_i = 500–600$ μV). In a weld seam, a large number of low-amplitude AE signals ($A_i = 200–250$ μV) are radiated.

A specific feature of the AE generation kinetics at the fatigue initiation stage is the fact that AE signals are radiated in certain groups, the sums of whose amplitudes are proportional to the formation of new surfaces at the crack front. An abrupt jump in the AE activity is observed upon the transition from the initiation stage to stable fracture propagation.

REFERENCES

1. Grondel, S., Delebarre, C., Assaad, J., et al., Fatigue crack monitoring of riveted aluminium strap joints by Lamb wave analysis and acoustic-emission measurement techniques, *NDT & E International,* 2002, vol. 35, pp. 137–146.
2. Duke, J.C. and Green, J., Simultaneous monitoring of acoustic emission and ultrasonic attenuation during fatigue of 7075 aluminum, *Int. J. Fatig.,* 1979, vol. 1, pp. 125–132.
3. Huang, M., Liang, J., Liaw, P.K., et al., Using acoustic emission in fatigue and fracture materials research, *JOM*, 1998, vol. 50, no. 11, pp. 1–12.

4. Harris, D.O. and Dunegan, H.L., Continuous monitoring of fatigue-crack growth by acoustic-emission techniques, *Experimental Mechanics*, 1974, vol. 14, no. 2, pp. 71–81.
5. Lindley, T.C., Palmer, I.G., and Richards, C.E., *Acoustic-emission monitoring of fatigue crack growth, Mater. Sci. Engineer.*, 1978, vol. 32, pp. 1–15.
6. Roberts, T., Talebzadeh, M., Acoustic-emission monitoring of fatigue crack propagation, *J. Construct. Steel Res.*, 2003, vol. 59, pp. 695–712.
7. Chang, H., Han, E.H., Wang, J.Q., et al., Acoustic emission study of fatigue crack closure of physical short and long cracks for aluminum alloy LY12CZ, *Int. J. Fatig.*, 2009, vol. 31, pp. 11–110.
8. Aggelis, D.G., Kordatos, E.Z., Matikas, T.E., et al., Acoustic emission for fatigue damage characterization in metal plates, *Mechan. Res. Commun.*, 2011, vol. 38, pp. 11–110.
9. Lee, C.K., Wilcocs, P.D., Drinkwater, B.W., et al., Acoustic emission during fatigue crack growth in aluminum plates, *Adv. Mater. Res.*, 2006, vol. 13–14, pp. 23–28.
10. Berkovits, A. and Fang, D., Study of fatigue crack characteristics by acoustic emission, *Engin. Fract. Mechan.*, 1995, vol. 51, pp. 401–409.
11. Fang, D. and Berkovits, A., Fatigue design model based on damage mechanisms revealed by acoustic emission measurements, *Trans. of the ASME,* 1995, vol. 117, pp. 200–208.
12. Scruby, C.B., Baldwin, G.R., and Stacey, K.A., Characterization of fatigue crack extension by quantitative acoustic emission, *Int. J. Fract.*, 1985, vol. 28, no. 4, pp. 201–222.
13. Scala, C.M. and Cousland, S., McK, Acoustic emission during fatigue crack propagation in the aluminum alloys 2024 and 2124, *Mater. Sci. Engin.*, 1983, vol. 61, pp. 211–218.
14. Baram, J. and Rosen, M., Prediction of low-cycle fatigue-life by acoustic emission–1: 2024-T3 aluminum alloy, *Engin. Fract. Mechan.*, 1981, vol. 15, pp. 487–494.
15. *GOST* (State Standard) *4784-97, Aluminum and deformed aluminum alloys. Grades*, Moscow: Mezhgosudarstv. Sovet standartiz., metrol. sertifik., 1997.
16. Skal'skii, V.R., Botvina, L.R., and Lyasota, I.M., Features of the structural and mechanical inhomogeneities in welded joints of the 1201-T alloy produced by electron-beam welding, *Avtomatich. Svarka*, 2012, no. 7, pp. 19–23.
17. *Metodicheskie ukazaniya. Problemy prochnosti, dolgovechnosti i nadezhnosti produktsii mashinostroeniya. Metody mekhanicheskikh ispytanii metallov. Opredelenie kharakteristik treshchinostoikosti pri tsiklicheskom nagruzhenii* (Methodological Instructions. Problems of Strength, Durability, and Reliability of Machine-Building Products. Methods for Mechanical Tests of Metals. Determining the Characteristics of Crack Resistance under Cyclic Loading), Moscow, 1993.
18. Skalskyi, V.R. and Koval, P.M., *Some methodological aspects of application of acoustic emission*, Lviv: Spolom, 2007.
19. Romaniv, O.N., Yarema, S.Ya., Nikiforchin, G.N., et al., *Mekhanika razrusheniya i prochnost' materialov. Ustalost' i tsiklicheskaya treshchinostoikost' konstruktsionnykh materialov* (Fracture Mechanics and Strength of Materials. Fatigue and Cyclic Crack Resistance of Structural Materials), Kiev: Nauk. dumka, 1990, vol. 4.
20. Skal's'kii, V.R., Lyasota. I.M., and Stankevich, O.M., Acoustic-emission diagnostics of fatigue failure in the 1201-T aluminum alloy, *Fiz.-Khim. Mekhan. Mater.*, 2012, no. 5, pp. 110–116.

Translated by A. Seferov